



Effect of siderophores on the light-induced dissolution of colloidal iron(III) (hydr)oxides

Paul M. Borer^a, Barbara Sulzberger^a, Petra Reichard^b, Stephan M. Kraemer^{b,*}

^aSwiss Federal Institute for Environmental Science and Technology (EAWAG), Überlandstrasse 133, 8600 Dübendorf, Switzerland

^bInstitute of Terrestrial Ecology, Swiss Federal Institute of Technology, Zürich, Grabenstrasse 3, 8952 Schlieren, Switzerland

Received 11 March 2004; received in revised form 23 August 2004; accepted 24 August 2004

Available online 14 October 2004

Abstract

Siderophores play an important role in biological iron acquisition in iron-limited aquatic systems. While it is widely accepted that the solubilization of iron-bearing mineral phases is a key function of siderophores, the mechanism of siderophore-promoted mineral dissolution in aquatic systems is largely unknown. In this study, we investigated the effect of siderophores (desferrioxamine B (DFOB) and aerobactin) on light-induced dissolution of goethite and lepidocrocite in the presence or absence of oxalate in aerated and deaerated suspensions at pH 6. For the irradiated two-ligand system (oxalate/siderophore), the experimental results suggest that oxalate acts as the electron donor for the formation of surface Fe(II), and the siderophore acts as an efficient shuttle for the transfer of surface Fe(II) into solution. Furthermore, even in the absence of an electron donor such as oxalate, both DFOB and aerobactin accelerated the light-induced dissolution of lepidocrocite as compared to the thermal dissolution. Experiments with dissolved Fe(III)–DFOB and Fe(III)–aerobactin complexes suggest that this enhancing effect is not due to photolysis of corresponding surface complexes but to efficient transfer of reduced surface Fe(II) into solution, where surface Fe(II) may be formed, e.g., through photolysis of surface Fe(III)–hydroxo groups. Based on this study, we conclude that the interplay of light and siderophores may play a key role in the dissolution of colloidal iron(III) (hydr)oxides in marine systems, particularly in the presence of efficient electron donors.

© 2004 Elsevier B.V. All rights reserved.

Keywords: Photodissolution; Iron oxides; Siderophore; Desferrioxamine B (DFOB); Aerobactin; Oxalate; Marine iron limitation

1. Introduction

Iron bioavailability has been shown to limit or colimit primary productivity in several oceanic waters,

particularly in ‘High Nutrient, Low Chlorophyll’ (HNLC) regions (Martin and Fitzwater, 1988; Martin et al., 1994). A significant external iron source to these and other oceanographic regimes is atmospheric input (Martin and Fitzwater, 1988; Martin et al., 1994). For example, it has been estimated that atmospheric deposition of aeolian iron-containing mineral dust accounts for 84–93% of the external iron input to the

* Corresponding author. Tel.: +41 1 633 6077; fax: +41 1 633 1118.

E-mail address: kraemer@env.ethz.ch (S.M. Kraemer).

subarctic Pacific, which lies in the path of an extended aerosol plume that originates in China (Martin et al., 1989). At the relatively low pH values (3–6) of atmospheric waters, solid iron phases (e.g., crystalline iron oxides and iron aluminium silicates) in the aerosols are subject to photoreductive dissolution (Faust and Hoffmann, 1986; Pehkonen et al., 1993; Zhu et al., 1993; Siefert et al., 1994; Sulzberger and Laubscher, 1995a,b; Johansen et al., 2000). Besides crystalline iron oxides (this term will be used for the various Fe(III) oxides, Fe(III) oxohydroxides, and Fe(III) hydroxides), photoproduct Fe(II) also enters open ocean surface waters by wet deposition. However, without significant stabilization of Fe(II) by some organic ligands, Fe(II) undergoes fast oxidative precipitation in seawater (Millero et al., 1987).

The extent to which iron limits primary production in open ocean waters depends on both the abundance of iron and its bioavailability. Particulate and colloidal iron is believed to be unavailable to phytoplankton (Wells et al., 1983; Finden et al., 1984; Rich and Morel, 1990), and the solubility of iron in open ocean waters is extremely low, $\log [\text{Fe(III)}] < -9$ (Liu and Millero, 2002). Regarding dissolved iron, it has been proposed that eukaryotic phytoplankton species utilize only inorganic iron species (Anderson and Morel, 1982). However, more recent studies have shown that some eukaryotic algae are able to utilize iron bound to (strong) organic chelators via a cell surface reductase mechanism (Jones et al., 1987; Soria-Dengg and Horstmann, 1995; Hutchins et al., 1999; Maldonado and Price, 1999, 2001; Weger, 1999).

Unlike eukaryotic algae, marine bacteria acquire iron through a siderophore-mediated uptake system (Winkelmann, 1991). Siderophores are low-molecular-weight organic ligands (0.5–1.5 kDa) with a high affinity and specificity for iron. Under iron-limiting conditions, siderophores are excreted by cyano- and heterotrophic bacteria (Gonye and Carpenter, 1974; Reid and Butler, 1991; Haygood et al., 1993; Wilhelm and Trick, 1994; Tortell et al., 1999). The stability constants of Fe(III)–siderophore complexes are in the range of $\log K = 25–50$ (Albrecht-Gary and Crumbliss, 1998). Besides increasing the solubility of iron, siderophores also accelerate iron oxide dissolution (Hersman et al., 1995; Yoshida et al., 2002; Cheah et al., 2003; Kraemer, 2004). Iron-binding groups of

bacterial siderophores typically include hydroxamate, catecholate, α -hydroxycarboxylate, and, less often, carboxylate groups (Winkelmann, 1991).

Hitherto, there is no clear picture of the roles of siderophores for iron acquisition by the phytoplankton community. The acquisition of iron from iron–siderophore complexes by eukaryotic phytoplankton (e.g., diatoms) is obscure and controversially discussed in literature. Although eukaryotic phytoplankton generally do not produce siderophores, it has been shown that some species may utilize siderophore-bound iron under iron-limiting conditions by a cell surface reductase mechanism (Soria-Dengg and Horstmann, 1995; Maldonado and Price, 2001). Other studies, however, have pointed out, that strong iron–siderophore complexes are not available to eukaryotic phytoplankton in iron-replete waters (Wells et al., 1994; Wells, 1999). For an in-depth discussion of these contrasting results, we refer to Maldonado and Price (2001).

It has been reported, that most (>99%) dissolved ferric iron in the HNLC upper ocean water is complexed by strong organic ligands having conditional stability constants in seawater similar to siderophores (Van den Berg, 1995; Wu and Luther, 1995; Rue and Bruland, 1997; Witter et al., 2000; Powell and Donat, 2001). The nature of these ligands has been partly elucidated by Macrellis et al. (2001). They have determined size classes as well as conditional Fe-binding affinities of iron binding compounds collected in the central California coastal upwelling system. The size class and conditional stability constants of these ligands were similar to known siderophores. Moreover, hydroxamate as well as catecholate Fe(III)-binding groups were found in all compounds for which strong iron binding was detected.

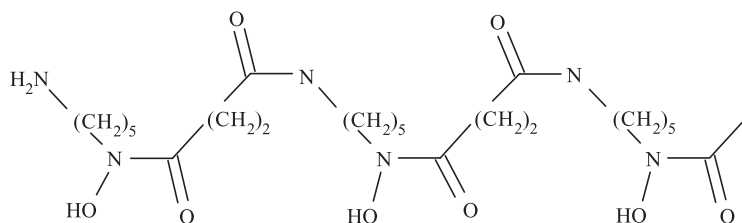
1.1. Roles of siderophores in the light-induced redox cycling of dissolved iron

The effect of siderophores on the redox chemistry of dissolved iron is dominated by two processes: (i) stabilization of the trivalent state of iron due to the much higher affinity of siderophores for Fe(III) compared to Fe(II), and (ii) photolysis of certain Fe(III)–siderophore complexes resulting in the formation of Fe(II). It has been demonstrated that Fe(III)

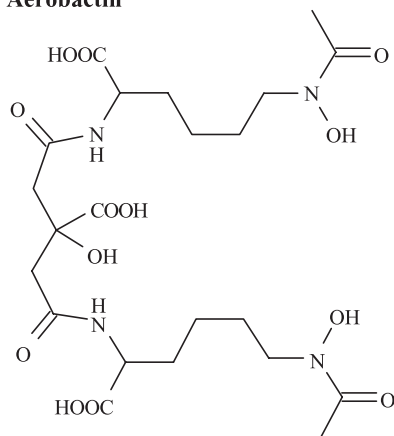
complexes with the marine siderophores petrobactin (Fig. 1; Barbeau et al., 2002) and that various aquachelins (Barbeau et al., 2001) are photolyzed under irradiation, yielding Fe(II), and increased bioavailability of iron to phytoplankton (as has been demonstrated for the photolysis of the Fe(III)–aquachelin B complex). The photoreactivity of Fe(III)–petrobactin and Fe(III)–aquachelin complexes is

imparted by the α -hydroxycarboxylate functional group which decarboxylates under irradiation. This is consistent with earlier observations of the photoreactivity of α -hydroxycarboxylic acids complexed to transition metals (Abrahamson et al., 1994; Kuma et al., 1995). According to a recent study of the photochemical reactivity of siderophores based on characteristic iron(III)-binding groups, siderophores

Desferrioxamine B (DFOB)



Aerobactin



Petrobactin

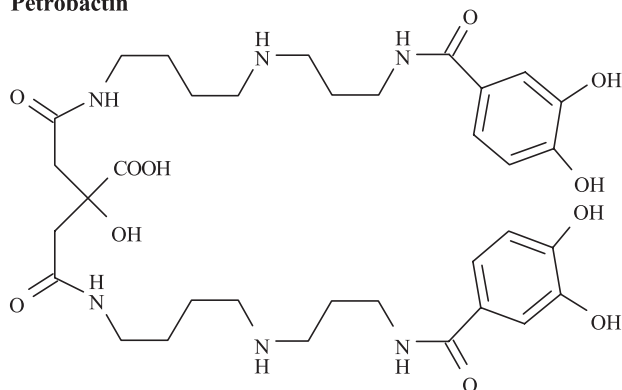


Fig. 1. Chemical structures of the microbial siderophores DFOB, aerobactin, and petrobactin (Bergeron et al., 2003).

containing only hydroxamate groups such as desferrioxamine B (DFOB; Fig. 1) form photostable iron complexes (Barbeau et al., 2003).

The stabilization of the trivalent redox state of iron by siderophores can be related to the stability constants of the Fe(II)- and Fe(III)-complexes (Taylor et al., 1994):

$$E_{\text{Fe}^{\text{III}}/\text{II}}^{\text{O}} = E_{\text{aq}}^{\text{O}} - 59.15 \log \left(\frac{\beta_{110}^{\text{Fe(III)}}}{\beta_{110}^{\text{Fe(II)}}} \right) \quad (1)$$

where the redox potential of the hexaaquated iron E_{aq}^{O} is +770 mV (vs. normal hydrogen electrode). Due to the much higher affinity of siderophores to Fe(III) than to Fe(II) ($\beta_{110}^{\text{Fe(III)}} \gg \beta_{110}^{\text{Fe(II)}}$), redox potentials observed for most Fe–siderophore complexes are in the range of –350 to –750 mV. These strongly negative redox potentials facilitate Fe(II) oxidation in the presence of oxygen. In the reported case of Fe(II)–DFOB complexes, the oxidation to Fe(III)–DFOB is instantaneous (Welch et al., 2002). Based on the above consideration, measured Fe(II) concentrations may not be a suitable indicator for photoreductive dissolution of iron oxides in the presence of siderophores in the laboratory or in marine in situ studies.

1.2. Roles of siderophores in the thermal dissolution of iron oxides

The dissolution of iron oxides requires the breaking of bonds between surface Fe(III) and lattice neighbors (e.g., lattice oxygen). Surface chemical processes that weaken these bonds can accelerate iron oxide dissolution. Protonation of surface sites, adsorption of ligands, and (photo)reduction of surface sites by reductive agents all lead to polarization of metal–oxygen bonds and therefore promote dissolution (Zinder et al., 1986).

Siderophores react with iron oxides in the dark via a ligand-controlled dissolution mechanism (Kraemer, 2004) with a rate law proposed by Furrer and Stumm (1986):

$$R_{\text{L}} = k_{\text{L}}[\text{L}]_{\text{ads}} \quad (2)$$

where R_{L} is the dissolution rate, k_{L} is a first-order rate constant, and $[\text{L}]_{\text{ads}}$ is the adsorbed ligand concentration. Siderophores also accelerate other ligand-

controlled dissolution mechanisms. A recent study of thermal steady-state dissolution kinetics of goethite in the presence of DFOB and oxalate at near neutral pH has revealed that the rate determining step in the overall dissolution reaction is the detachment of surface Fe(III) by oxalate, followed by a ligand exchange reaction between DFOB– and Fe(III)–oxalate complexes in solution (Cheah et al., 2003).

1.3. Mechanism and rate law of light-induced dissolution of iron oxides

Photodissolution of iron oxides has been subject to many studies (Waite and Morel, 1984; Faust and Hoffmann, 1986; Litter and Blesa, 1988; Siffert and Sulzberger, 1991; Pehkonen et al., 1993; Sulzberger and Laubscher, 1995a,b). The dissolution process generally involves two steps:

1. Photoexcitation and charge transfer resulting in the reduction of surface Fe(III) to Fe(II).
2. Detachment of reduced surface Fe(II) from the mineral surface.

Different mechanisms can result in the formation of surface Fe(II): (i) ligand-to-metal charge transfer (LMCT) within organic Fe(III) surface complexes or within surface Fe(III)–hydroxo groups, leading to the reduction of surface Fe(III) and the oxidation of the ligand, and (ii) generation of photoelectrons and photoholes within the iron oxide lattice (semiconductor mechanism) through photoexcitation of $\text{O}^{2-} \rightarrow \text{Fe}^{3+}$ charge transfer bands and migration of photoelectrons to surface Fe(III) and photoholes to an adsorbed electron donor. (Di)carboxylate and hydroxycarboxylate functional groups are important electron donors and are ubiquitous in biogenic organic compounds. Furthermore, (di)carboxylic and hydroxycarboxylic acids are also introduced to remote ocean surface waters by wet deposition of photochemically transformed anthropogenic precursors (Sempere and Kawamura, 1996, 2003).

Irrespective of the mechanism involved, the rate-determining step in the dissolution of crystalline iron oxides is the detachment of Fe(II) from the mineral surface (Banwart et al., 1989; Siffert and Sulzberger, 1991; Stumm and Sulzberger, 1992), and the rate of Fe(II) formation is linearly dependent on the concen-

tration of the adsorbed ligand, acting as electron donor (see Eq. (2)). In the presence of oxygen and depending on pH, detachment of reduced surface iron may be outcompeted by reoxidation of surface Fe(II). Unless stabilized by ligands, detached Fe(II) is subject to oxidative precipitation in circumneutral surface waters, resulting in the formation of amorphous iron oxide phases (Wells and Mayer, 1991). These freshly formed amorphous iron oxide phases are more readily dissolved than crystalline iron oxides. Hence, photo-reductive dissolution is an important process, potentially increasing the bioavailability of iron in circumneutral surface waters (Finden et al., 1984; Wells and Mayer, 1991; Johnson et al., 1994; Miller and Kester, 1994).

1.4. Purpose of this study

Solubilization of crystalline iron oxides originating from tropospheric deposition increases the pool of iron that may be available to the marine biota. Several studies have shown that photoreductive dissolution of crystalline iron oxides phases in the presence of humic substances or model compounds such as oxalate, acting as electron donors, is extremely slow above acidic pH values (Waite and Morel, 1984; Sulzberger and Laubscher, 1995a; Voelker et al., 1997). Hitherto, the effect of siderophores on photoreductive dissolution has not yet been studied. Although we did not attempt to mimic natural conditions in iron deficient areas of the open ocean, we have investigated the interplay of siderophores and oxalate in photodissolution of iron oxides. In this study, we worked with two model siderophores: DFOB, a trihydroxamate siderophore, and aerobactin, a dihydroxamate/ α -hydroxycarboxylate siderophore (Fig. 1).

2. Materials and methods

2.1. Materials

Desferrioxamine B was obtained as mesylate salt [$C_{25}H_{46}N_5O_8NH_3^+(CH_3SO_3^-)$] from Ciba Geigy (Desferal®). Iron-free aerobactin ($C_{22}H_{32}O_{12}N_4$) was purchased from EMC microcollections in Tübingen, Germany and used as received. All other chemicals were reagent grade and solutions were

prepared with high purity $18.2 \text{ M}\Omega \text{ cm}^{-1}$ water (Milli-Q, Millipore). pH measurements were carried out with a combined glass electrode (Metrohm), standardized with pH-buffer solutions (Merck). Goethite (α -FeOOH) was synthesized using a method described by Schwertmann and Cornell (1991), dialyzed, and freeze-dried. Lepidocrocite (γ -FeOOH) was prepared according to a procedure developed by Brauer (1963) by oxidation of $FeCl_2$ with $NaNO_2$ in the presence of hexamethylenetetraamine at 60°C for 3 h. In order to remove excess chloride, the lepidocrocite suspension was washed several times by centrifugation and resuspension in high purity water. The precipitate was freeze-dried. Powder X-ray diffraction confirmed that the synthesized solids are goethite and lepidocrocite. The specific surface area as determined by the BET method is $170 \text{ m}^2/\text{g}$ for lepidocrocite and $38 \text{ m}^2/\text{g}$ for goethite. The point of zero charge (PZC) of lepidocrocite produced according to the method by Brauer is 7.5 (Bondiotti, 1992). For goethite, an isoelectric point (IEP) of 8.3 was determined by measuring the electrophoretic mobility of suspended particles.

2.2. Dissolution experiments

Dissolution experiments were performed with two experimental systems. The first setup (solar simulator) consisted of a 1000-W, high-pressure xenon lamp (OSRAM), from which the originating light (spectrum similar to that of sunlight) was filtered by the bottom window of the Pyrex glass vessel acting as a cutoff filter at 305 nm (Siffert and Sulzberger, 1991). All experiments were carried out in a Pyrex glass vessel with a water jacket at constant temperature ($25 \pm 1^\circ\text{C}$). The incident light intensity, I_0 , was 1200 W/m^2 , as measured by ferrioxalate actinometry. The reaction volume was typically 350 ml and the irradiated surface area was 50 cm^2 . The solutions were vigorously stirred with a Teflon-coated stirrer. The ionic medium used for the dissolution experiments was 0.01 M $KClO_4$. Suspensions of 0.08 g/L goethite or 0.02 g/L lepidocrocite were irradiated for several hours in the presence of $80 \mu\text{M}$ DFOB and/or $200 \mu\text{M}$ K-oxalate. Goethite suspensions including organic ligands were prepared 17 h before irradiation and stored in the dark to circumvent thermal fast initial dissolution reactions during irradiation experiments.

By adding appropriate amounts of diluted HCl or NaOH, the pH of the solutions was kept constant at pH 6 during the entire experiments. Two different types of experiments were performed: steady-state experiments, in which DFOB and oxalate were both added to goethite or lepidocrocite suspensions before irradiation; and non-steady-state experiments in which oxalate reacted with the iron oxides under irradiation before adding DFOB. Oxygen-free (deaerated) conditions were maintained by purging N₂ through the suspensions and sporadically applying a weak vacuum.

The second experimental setup was a light box equipped with eight Philips TL20W/05 lamps (spectrum ranging from 300 to 460 nm with a maximum at 365 nm) on two opposite sides inside the box. Dissolution experiments were carried out in 4-ml polymethylmethacrylat (PMMA) cuvettes with two optical sides with excellent transmission in the range of 280–800 nm. The cuvettes with dimensions of 1 cm×1 cm×4 cm were always placed on a magnetic stirrer plate at the same height. Because light transmission also occurred through the two non-optical sides of the cuvettes, an incident light intensity I_0 of approximately 55 W/m² was estimated by ferrioxalate actinometry. An average photolysis quantum yield of 1.16 was used for the light intensity calculation. Suspensions containing 0.02 g/L lepidocrocite, 0.01 M KClO₄, and 45 μM DFOB or aerobactin at pH 6 were irradiated for over 4 h. The suspensions were stirred with small magnet bars. An integrated ventilator kept the temperature at about 32 to 34 °C. Dark experiments were carried out at the same temperature in a temperature-controlled water bath.

In all dissolution experiments, samples of the suspensions were periodically taken, immediately filtered, and acidified with a small amount of 65% suprapure HNO₃ (Merck). Single-use syringe filters with 0.2-μm pore size (Sartorius) were used for goethite suspensions. Preliminary tests showed that significant fractions of a lepidocrocite suspension passed through membrane filters with 0.2-μm pore size. Therefore, membrane filters with a pore size of 0.025 μm (Schleicher and Schuell) were used to filter lepidocrocite suspensions. We operationally define iron that passes through these filters as total dissolved iron [Fe_{tot}]. Total dissolved iron was measured by

ICP-MS (Agilent 7500 Series; iron standards from Fluka).

2.3. Photolysis of dissolved Fe(III)–siderophore complexes

Solutions of 45 μM 1:1 Fe(III)–DFOB and 1:1 Fe(III)–aerobactin complexes were prepared by adding the equivalent amount of siderophore to a solution of 45 μM FeCl₃·6H₂O at pH 1. The pH of the solutions was varied by titrating these unbuffered solutions manually with NaOH. No electrolyte was added. The ionic strength of solutions with pH>3 was approximately 0.1 M due to the initial acidification to pH 1 with HCl and titration with NaOH back to higher pH. Light and dark experiments were performed with the second experimental setup. UV-visible absorption of the irradiated and nonirradiated solutions were recorded with a UV-visible spectrophotometer (Cary 1E) using a microcuvette (5-cm path length, 0.7-ml volume). Analogous experiments were carried out with 0.15 g/L lepidocrocite suspensions in the presence of 45 μM aerobactin and 0.01 M KClO₄. After irradiation, samples were filtered and the spectra of the filtered solutions were recorded.

3. Results

3.1. Photolysis of Fe(III)–siderophore complexes in homogeneous and heterogeneous systems

Aqueous Fe(III)–aerobactin complexes exhibited pH-dependent peak shifts in the UV-visible spectrum consistent with published results (Harris et al., 1979). Decreasing the pH from 6 to 3.5 led to a shift of the absorption peak maximum from 395 to about 430 nm. Similar peak shifts were observed upon irradiation of a solution of 1:1 Fe(III)–aerobactin at a constant pH of 6.3 for 2 and 6 h (Fig. 2), whereas the spectrum of the nonirradiated Fe(III)–aerobactin solution did not change over time. The irradiated solution (pH 6.3) exhibited a UV-visible spectrum similar to that of a nonirradiated solution at pH 3.5 (with absorption maximum at 430 nm), which is consistent with a light-induced change in the coordination sphere of Fe(III)–aerobactin

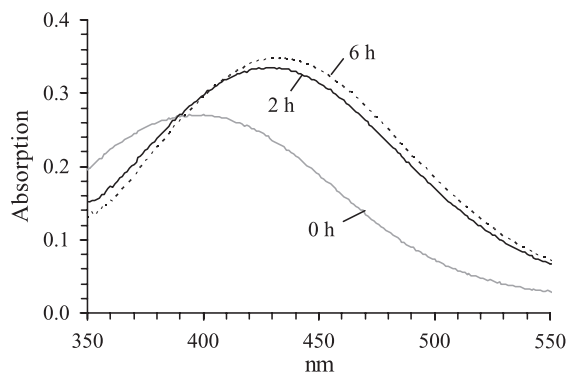


Fig. 2. UV-visible spectra of 1:1 Fe(III)-aerobactin complexes (45 μM) irradiated for 2 and 6 h or kept in the dark. $I_0=55 \text{ W/m}^2$ (blue actinic light source with a spectral range between 300 and 460 nm). $T=32 \text{ }^\circ\text{C}$, pH 6.3, and ionic strength of $\sim 0.1 \text{ M}$.

complexes analogous to the pH-dependent change in the coordination sphere. We have also observed peak shifts in irradiated solutions of Fe(III)-aerobactin complexes at lower pH. At pH 5, a peak shift from 402 to 427 nm occurred upon irradiation, whereas at pH 4, a peak shift from 423 to 430 nm was observed. Irradiation of a Fe(III)-DFOB solution for 6 h at pH 6 did not result in changes in the UV-visible absorption spectra (data not shown), which is in agreement with recent reports (Barbeau et al., 2003).

To investigate photolysis of Fe(III)-aerobactin complexes at the lepidocrocite surface, lepidocrocite suspensions were irradiated in the presence of

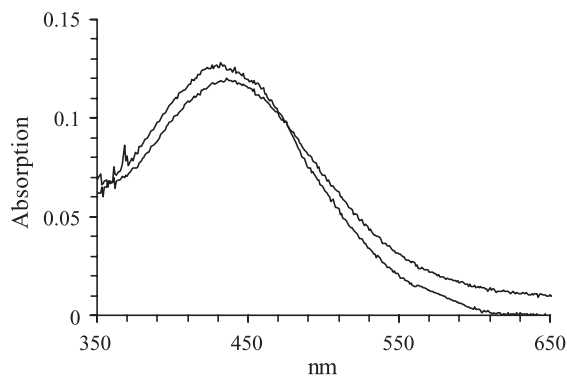


Fig. 3. UV-visible spectra of two filtered suspensions (independent replicates) containing 0.15 g/L lepidocrocite and 45 μM aerobactin, after 6 h irradiation with $I_0=55 \text{ W/m}^2$ (blue actinic light source with a spectral range between 300 and 460 nm). $T=32 \text{ }^\circ\text{C}$, pH 6, electrolyte=0.01 M KClO_4 .

aerobactin for 6 h at pH 6. The spectra of two filtered solutions (independent replicates) showed an absorption maxima at 430 nm (Fig. 3) which also was found for an irradiated homogeneous Fe(III)-aerobactin solution at pH 6.3 (Fig. 2).

3.2. Effects of DFOB or aerobactin and light on the dissolution of lepidocrocite and goethite

The results of lepidocrocite dissolution experiments in the presence of aerobactin or DFOB are shown in Fig. 4. No significant dissolution was observed in the absence of these siderophores, even in a deaerated, irradiated lepidocrocite suspension. Thermal lepidocrocite dissolution rates were accelerated in the presence of DFOB and aerobactin (2.0 and 2.8 $\text{nmol min}^{-1} \text{ m}^{-2}$, respectively). Irradiation caused further acceleration of dissolution rates relative to thermal dissolution rates by a factor of four and six (8.2 and 11.5 $\text{nmol min}^{-1} \text{ m}^{-2}$) in the presence of DFOB and aerobactin, respectively.

No thermal or photodissolution of goethite was observed in the presence of DFOB as the only organic ligand (detection limit $\sim 0.1 \mu\text{M Fe}$) under aerated or deaerated conditions on the time scale of the dissolution experiments (data not shown).

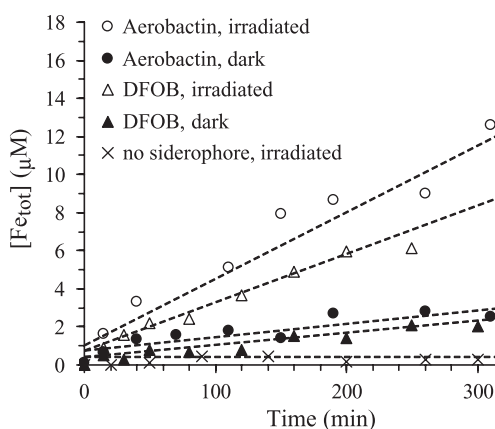


Fig. 4. Dissolution in aerated 0.02 g/L lepidocrocite suspensions in the presence of 45 μM aerobactin or DFOB. Suspensions were either irradiated with $I_0=55 \text{ W/m}^2$ (blue actinic light source with a spectral range between 300 and 460 nm) or kept in the dark. Lepidocrocite suspensions (deaerated) were also irradiated in the absence of siderophores. $T=32 \text{ }^\circ\text{C}$, pH 6, electrolyte=0.01 M KClO_4 . $[\text{Fe}_{\text{tot}}]$ =total dissolved iron measured by ICP-MS.

Table 1

Dissolution rates in irradiated lepidocrocite suspensions at pH 6 in the presence of DFOB and/or oxalate (0.02 g/L lepidocrocite, electrolyte=0.01 M KClO₄; T=25 °C, I₀=1200 W/m²)

[DFOB] (μM)	[Oxalate] (μM)	Deaerated	Dissolution rate (nmol m ⁻² min ⁻¹)
–	–	No	n.d.
–	–	Yes	n.d.
80	–	No	5.4
80	–	Yes	7.3
–	200	No	Small, nonlinear
–	200	Yes	11.8
80	200	No	~24.3
80	200	Yes	~24.3

n.d.: no detectable increase in iron concentrations over the course of the dissolution experiment.

3.3. Photodissolution of lepidocrocite and goethite in the presence of DFOB and/or oxalate

Dissolution rates of lepidocrocite in the presence or absence of DFOB and oxalate are summarized in Table 1 and Fig. 5. Under aerated conditions at pH 6, oxalate did not promote significant photodissolution, whereas DFOB did (see also Fig. 4). However, under deaerated, irradiated conditions, appreciable dissolution rates were observed in the presence of oxalate only. Photodissolution of lepidocrocite under aerated conditions was greatly enhanced by DFOB when oxalate also was present. There was no significant

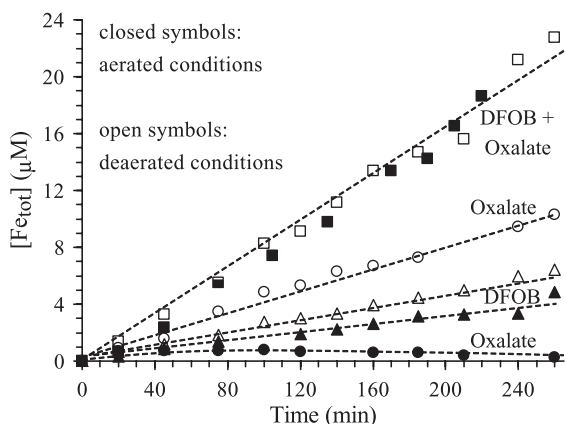


Fig. 5. Dissolution in irradiated 0.02 g/L lepidocrocite suspensions in the presence/absence of 80 μM DFOB/200 μM oxalate. I₀=1200 W/m² (xenon lamp with a spectral range between 300 and 800 nm), T=25 °C, pH 6, electrolyte=0.01 M KClO₄. Closed symbols stand for aerated suspensions, open symbols for deaerated suspensions. [Fe_{tot}]=total dissolved iron measured by ICP-MS.

Table 2

Dissolution rates in irradiated goethite suspensions at pH 6 in the presence of DFOB and/or oxalate (0.08 g/L goethite, electrolyte=0.01 M KClO₄; T=25 °C, I₀=1200 W/m²)

[DFOB] (μM)	[Oxalate] (μM)	Deaerated	Dissolution rate (nmol m ⁻² min ⁻¹)
80	–	No	n.d.
80	–	Yes	n.d.
–	200	No	n.d.
–	200	Yes	n.d.
80	200	No	0.59
80	200	Yes	2.9

n.d.: no detectable increase in iron concentrations over the course of the dissolution experiment.

difference in photodissolution rates in the two-ligand system under aerated and deaerated conditions.

Results of goethite dissolution experiments are summarized in Table 2 and Fig. 6. The dissolution rates were generally lower than those observed for lepidocrocite under the same conditions. For example, the lepidocrocite dissolution rate in the presence of 80 μM DFOB and 200 μM oxalate in the dark was 6.2 nmol m⁻² min⁻¹, and, hence, more than an order of magnitude higher than the corresponding dissolution rate for goethite (0.1 nmol m⁻² min⁻¹). Furthermore, no thermal dissolution or photodissolution of goethite was observed in the presence of either DFOB or oxalate on the time scale of the experiments. Only for goethite suspensions containing both DFOB and

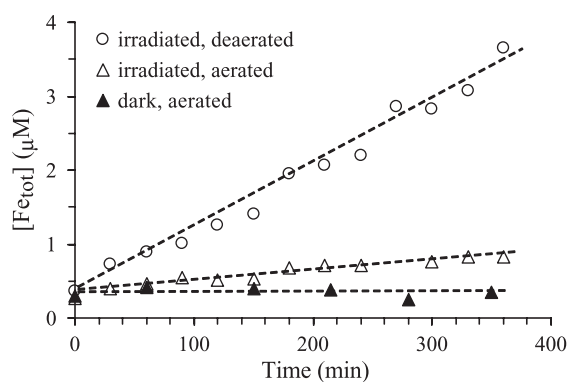


Fig. 6. Dissolution in 0.08 g/L goethite suspensions in the presence of 80 μM DFOB and 200 μM oxalate under different conditions. I₀=1200 W/m² (xenon lamp with a spectral range between 300 and 800 nm), T=25 °C, pH 6, electrolyte=0.01 M KClO₄. Suspensions were kept first for 17 h in the dark to circumvent fast dissolution during irradiation experiments. After this time span, total dissolved iron concentrations as measured by ICP-MS were 0.3–0.4 μM.

oxalate, dissolution rates were increased upon irradiation and dissolution rates were smaller in aerated than in deaerated suspensions (Fig. 6). As mentioned above, oxygen had no effect on light-induced dissolution rates of lepidocrocite in the presence of both DFOB and oxalate (Fig. 5).

3.4. Non-steady-state experiments with lepidocrocite and goethite in the two-ligand system DFOB/oxalate

To investigate whether kinetically labile surface sites (e.g., photoproducted Fe(II), or freshly formed iron oxide phases) accumulate at the mineral surface in the presence of oxalate, we conducted non-steady-state experiments. Deaerated or aerated lepidocrocite and goethite suspensions were first exposed to oxalate for a few hours, before adding a spike of DFOB. In Fig. 7A–C, the dissolution kinetics in non-steady-state experiments is compared to that in the steady-state experiments, in which DFOB and oxalate were added simultaneously to lepidocrocite or goethite suspensions. As soon as DFOB was added to irradiated, lepidocrocite (aerated) and goethite (deaerated) suspensions containing oxalate (at 70 and 200 min, respectively), the dissolution rate equaled that of the corresponding steady-state experiment (Fig. 7A, B). Hence, on the time scale of this experiment, we observed no accumulation of kinetically labile surface sites in irradiated suspensions at pH 6.

Goethite suspensions were first conditioned in the dark for 17 h with oxalate and oxalate/DFOB in non-steady-state and steady-state experiments, respectively, before irradiating the suspensions. Within this conditioning period, no detectable thermal dissolution by oxalate took place, whereas thermal dissolution was obvious in the presence of both oxalate and DFOB, resulting in dissolved iron concentrations of 0.3–0.4 μM (at 0 min) in deaerated and aerated suspensions (Fig. 7B, C). In irradiated, aerated goethite suspensions (Fig. 7C), the addition of DFOB led to fast initial dissolution which then slowed down to match the steady-state dissolution rate. No photodissolution was observed in aerated goethite suspensions before DFOB was added. The fast release of 0.3–0.4 μM dissolved iron after the addition of DFOB can be rationalized in terms of thermal formation of kinetically labile surface iron by oxalate during the

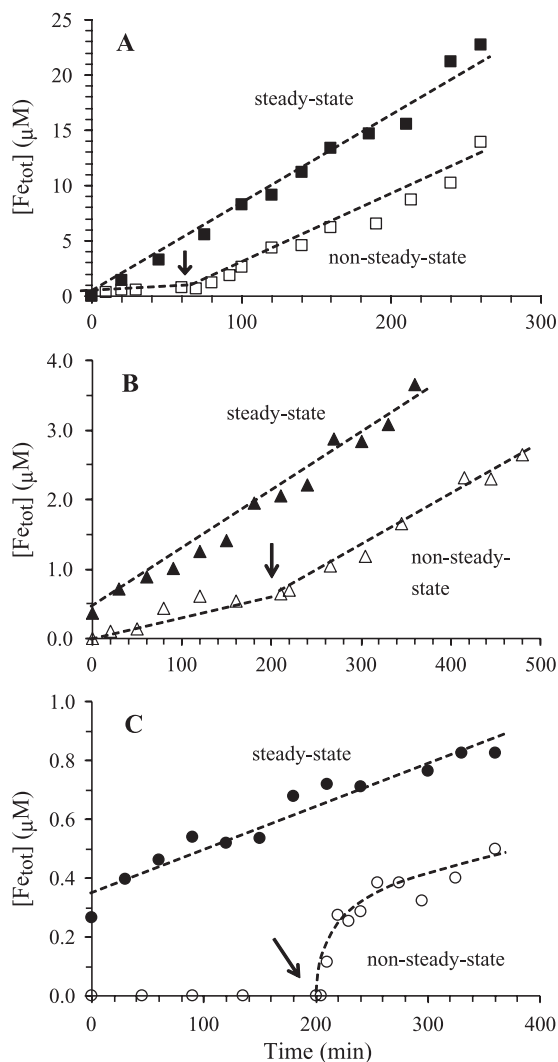


Fig. 7. Comparison of steady-state dissolution and non-steady-state dissolution in irradiated 0.02 g/L lepidocrocite suspensions (A) and 0.08 g/L goethite suspensions (B and C). In steady-state experiments, 80 μM DFOB and 200 μM oxalate were added simultaneously to the iron oxide suspensions, whereas in non-steady-state experiments, oxalate was first left to react with the iron oxides, before DFOB was added (at 70 and 200 min for lepidocrocite and goethite suspensions, respectively). (A) Aerated and irradiated lepidocrocite suspensions; (B) deaerated and irradiated goethite suspensions; (C) aerated and irradiated goethite suspensions. $T=25$ $^{\circ}\text{C}$, pH 6, $I=1200$ W/m^2 (xenon lamp with a spectral range between 300 and 800 nm), electrolyte=0.01 M KClO_4 . Goethite suspensions were kept first for 17 hours in the dark to circumvent fast dissolution during irradiation experiments. After this conditioning phase, total dissolved iron concentrations as measured by ICP-MS were 0.3–0.4 μM for steady-state experiments and 0 μM for non-steady-state experiments in panels (B) and (C).

conditioning phase and by the efficient detachment after the addition of DFOB at 200 min.

4. Discussion

4.1. Photolysis of Fe(III)–siderophore complexes

We measured UV-visible absorption spectra of Fe(III)–siderophore complexes before and after irradiation in order to investigate the photoreactivity of these complexes. Irradiation of 1:1 Fe(III)–aerobactin solutions at pH 4, 5, and 6.3 led to light-induced peak shifts in the absorption spectra with a final absorption maximum at approximately 430 nm (for pH 6.3 solution, see Fig. 2). These peak shifts clearly indicate the photoreactivity of dissolved Fe(III)–aerobactin complexes. It is likely that the photoreactivity of aerobactin is imparted by the α -hydroxycarboxylate-binding group. This suggests that the coordination of Fe(III) by both oxygen atoms of the hydroxyl and carboxyl moieties of the α -hydroxycarboxylate group is a prerequisite for photolysis to occur. We hypothesize that photolysis of the Fe(III)–aerobactin complex is likely to result in the destruction of the α -hydroxycarboxylate group and the formation of a 3-

Table 3
Thermodynamic stability constants at 25 °C and infinite dilution

Reaction	Log K_{298}^a
Aerobactin ⁵⁻ +H ⁺ =HAerobactin ⁴⁻	10.51
Aerobactin ⁵⁻ +2H ⁺ =H ₂ Aerobactin ³⁻	20.30
Aerobactin ⁵⁻ +3H ⁺ =H ₃ Aerobactin ²⁻	25.25
Aerobactin ⁵⁻ +4H ⁺ =H ₄ Aerobactin ⁻	29.16
Aerobactin ⁵⁻ +5H ⁺ =H ₅ Aerobactin	32.49
Aerobactin ⁵⁻ +Fe ³⁺ =FeH ₋₁ Aerobactin ³⁻ +H ⁺	20.67
Aerobactin ⁵⁻ +Fe ³⁺ =FeAerobactin ²⁻	25.72
Aerobactin ⁵⁻ +Fe ³⁺ +H ⁺ =FeHAerobactin ⁻	29.75
Aerobactin ⁵⁻ +Fe ³⁺ +2H ⁺ =FeH ₂ Aerobactin	33.06
Aerobactin ⁵⁻ +Fe ³⁺ +3H ⁺ =FeH ₃ Aerobactin ⁺	35.46
Fe ³⁺ +OH ⁻ =FeOH ²⁺	11.81
Fe ³⁺ +2OH ⁻ =Fe(OH) ₂ ⁺	23.4
Fe ³⁺ +3OH ⁻ =Fe(OH) ₃ (aq)	30.2
Fe ³⁺ +4OH ⁻ =Fe(OH) ₄ ⁻	34.4
2Fe ³⁺ +2OH ⁻ =Fe ₂ (OH) ₂ ⁴⁺	25.14
3Fe ³⁺ +4OH ⁻ =Fe ₃ (OH) ₄ ⁵⁺	49.7

FeH₋₁Aerobactin³⁻ is the photoreactive species [Fe³⁺(aerobactin⁶⁻)]³⁻.

^a Values are taken from Martell et al. (2001) and were corrected to zero ionic strength using the Davies equation.

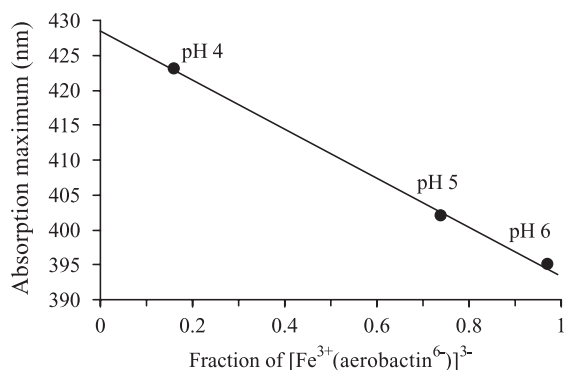


Fig. 8. Observed absorption maxima of non-irradiated solutions of 1:1 Fe(III)–aerobactin complexes (45 μ M) at different pH vs. the calculated fraction of the [Fe³⁺(aerobactin⁶⁻)]³⁻ species. The program CHEAQS vers. L19 was used for speciation calculations (Verweij, 1999–2001).

ketoglutarate residue in analogy to the structurally similar petrobactin (see Fig. 1; Barbeau et al., 2002). The changes in absorption spectra of the Fe(III)–aerobactin complex therefore reflect the loss of iron coordination by the α -hydroxycarboxylate group. This interpretation is supported by similar spectral changes due to pH shifts and hence changes of the coordination sphere of Fe(III)–aerobactin complexes. Harris et al. (1979) have observed UV-visible absorption spectra of Fe(III)–aerobactin complexes as a function of pH and concluded that pH-dependent shifts are due to changes in the coordination of iron by the citrate moiety. Raising solution pH from 3.5 to 6 increases the fraction of [Fe³⁺(aerobactin⁶⁻)]³⁻, in which Fe(III) is coordinated by both hydroxamate-binding groups, as well as the hydroxyl and carboxyl moieties of the α -hydroxycarboxylate group. According to speciation calculations, the fraction of this species constitutes 16%, 74%, and 97% at pH 4.0, pH 5.0, and pH 6.0, respectively, in 1:1 Fe(III)–aerobactin solutions ($I=0.1$ M). Thermodynamic data for the speciation calculation are listed in Table 3. A linear relationship between the pH-dependent fraction of [Fe³⁺(aerobactin⁶⁻)]³⁻ and the observed absorption peak maximum is found in nonirradiated 1:1 Fe(III)–aerobactin solutions (Fig. 8). At pH 3.5, the absorption peak maximum lies at approximately 430 nm, whereas at pH 6, the peak maximum occurs at 395 nm. Irradiation of 1:1 Fe(III)–aerobactin solutions with pH>3.5 leads to a peak shift to 430 nm, indicating photodegradation of the citrate moiety in

the photoreactive species $[\text{Fe}^{3+}(\text{aerobactin}^{6-})]^{3-}$ and hence loss of one binding group.

We have not observed changes in the UV-visible spectra of Fe(III)-DFOB complexes due to irradiation. This is consistent with previous reports on the photostability of Fe(III)-DFOB complexes (Barbeau et al., 2003).

4.2. Thermal and photodissolution of lepidocrocite by DFOB and aerobactin

The rate of siderophore-controlled iron oxide dissolution is influenced by the configuration and bonding of Fe–siderophore surface complexes. Similar rate constants of ligand-promoted dissolution of goethite in the presence of the trihydroxamate siderophore DFOB or monohydroxamate aHA (aceto-hydroxamic acid, see Fig. 9) have been reported (Cocozza et al., 2002). These authors have therefore concluded that only one hydroxamate group of DFOB participates in the formation of a bidentate mononuclear surface complex on goethite. In the case of aerobactin, the α -hydroxycarboxylate moiety as well as the hydroxamate moieties may participate in surface complex formation. The affinities of these functional groups for inner-sphere coordination of Fe(III) at the mineral surface are not known, but may be assessed from the stability constants of aqueous complexes of analogous compounds (Stumm et al., 1980). The overall stability constant of a typical 1:1 Fe(III)–monohydroxamate complex is much higher than that of an equivalent 1:1 Fe(III)– α -hydroxycarboxylate complex (Fig. 9). For example, the stability constant of 1:1 Fe(III)–aceto-hydroxamic acid (monohydroxamate complex) is eight orders of magnitude higher than that of 1:1 Fe(III)–glycolic acid (α -

hydroxycarboxylate complex; Martell et al., 2001). Therefore, we assume that weaker inner-sphere surface complexes are formed with α -hydroxycarboxylate-binding groups than with hydroxamate-binding groups and that hydroxamate groups will have a stronger effect on dissolution rates than α -hydroxycarboxylate groups. Such a correlation between ligand affinity and dissolution rates of iron oxides has been observed by Duckworth and Martin (2001). They have studied surface complexation and dissolution of hematite by various dicarboxylic acids at pH 5 and have observed a linear relationship between the ligand-promoted dissolution rate constants and the Langmuir binding constants. Based on above considerations, we propose surface coordination of aerobactin on iron oxides by a hydroxamate-binding group. The hypothesis that the α -hydroxycarboxylate group does not participate in surface complexation is consistent with the observation of equal light-induced and thermal lepidocrocite dissolution rates by DFOB and aerobactin (Fig. 4), despite the different photoreactivity of dissolved Fe(III)–aerobactin and Fe(III)–DFOB complexes. This indicates that both siderophores coordinate surface Fe(III) with the hydroxamate group and not with the α -hydroxycarboxylate group in the case of aerobactin, and that both siderophores do not promote photoreduction of Fe(III) surface sites by a ligand-to-metal charge transfer mechanism. UV-visible absorption spectra of filtered lepidocrocite suspensions that were irradiated in the presence of aerobactin (Fig. 3) exhibited the same spectral features as photolyzed Fe(III)–aerobactin complexes in solution (Fig. 2), typically having an absorption maximum at 430 nm. Most likely, the transfer of surface iron into solution occurs via the hydroxamate-binding group of aerobactin, and once dissolved Fe(III) is fully coordinated, photolysis of the Fe(III)–aerobactin complex occurs.

Possible mechanisms of Fe(III) photoreduction at the lepidocrocite surface in the presence of DFOB or aerobactin are photolysis of surface Fe(III)–hydroxo groups or excitation of the $\text{O}^{2-} \rightarrow \text{Fe}^{3+}$ charge-transfer bands with subsequent migration of the generated photoelectron to the oxide surface. Irrespective of the exact photochemical mechanisms that lead to the formation of surface Fe(II), both DFOB and aerobactin clearly promote the transfer of iron to the solution. This is consistent with the acceleration of the

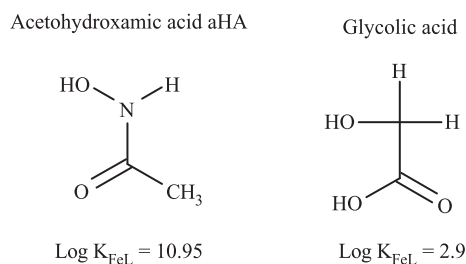


Fig. 9. Chemical structures of acetohydroxamic acid and glycolic acid and the stability constants (Martell et al., 2001) of aqueous 1:1 Fe(III)–ligand complexes at ionic strength $I=1$ M and 25 °C.

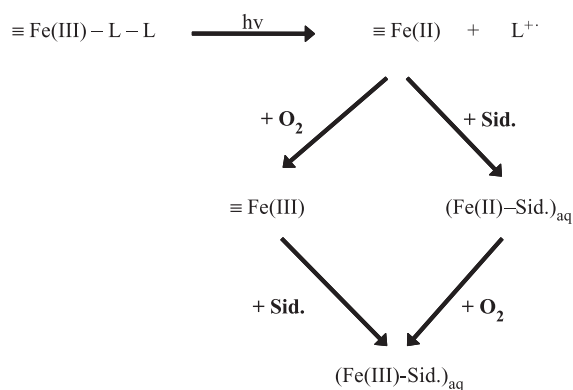
rate-determining detachment of Fe(II) in ligand-promoted, reductive dissolution (Banwart et al., 1989).

4.3. Thermal and photodissolution of goethite and lepidocrocite in the two-ligand system DFOB/oxalate

Oxalate is known to form photoreactive surface complexes at goethite and lepidocrocite surfaces and to promote fast photodissolution in the absence of oxygen (Siffert and Sulzberger, 1991; Sulzberger and Laubscher, 1995b). In the presence of oxygen and depending on pH, reoxidation of Fe(II) at the mineral surface may outcompete detachment of Fe(II) (Sulzberger and Laubscher, 1995a,b). In our study, the presence of oxygen reduced the rate of lepidocrocite photodissolution in the presence of oxalate to less than 50% relative to dissolution rates of deaerated suspensions at pH 6 (Fig. 5 and Table 1). This indicates that fast reoxidation of surface Fe(II) in aerated suspensions outcompetes its slow detachment from the lepidocrocite surface. However, in the presence of both oxalate and DFOB, photodissolution of lepidocrocite was significantly accelerated with similar rates in aerated and deaerated suspensions (Fig. 5). Considering that DFOB does not act as an electron donor (see discussion above), we conclude that DFOB is an efficient shuttle for the transfer of surface Fe(II) into solution.

The presence of oxygen has a bigger impact on light-induced dissolution of goethite in the presence of DFOB and oxalate (Fig. 6), as compared to lepidocrocite. This can be explained in terms of different thermodynamic stabilities of these two iron oxide phases. With goethite, detachment of reduced iron is likely to be slower than with lepidocrocite, resulting in competitive reoxidation of Fe(II) (Sulzberger and Laubscher, 1995b). These authors have reported that no dissolution took place in irradiated, aerated goethite and hematite suspensions at pH 3. However, as shown in Fig. 6, photodissolution of goethite does take place in aerated suspensions, even at pH 6, if DFOB is added to the system. The likely role of siderophores in the formation of dissolved iron through photoreductive dissolution of iron oxides is shown schematically in Fig. 10.

To investigate, if kinetically labile sites (Fe(II) and reoxidized surface sites) accumulate at irradiated



L = OH, photoreductive ligand

Fig. 10. General mechanism of light-induced dissolution in the presence of siderophores. Following photoexcitation of surface hydroxo complexes or surface ligand complexes and charge transfer, surface Fe(III) is reduced to Fe(II). For simplicity, the $\text{O}^{2-} \rightarrow \text{Fe}^{3+}$ semiconductor charge transfer mechanism is omitted. Detachment of Fe(II) is the rate determining step in the overall photodissolution reaction. A competing reaction is the reoxidation of surface Fe(II). Depending on the thermodynamic stability of the iron oxide, siderophore-promoted detachment may or may not outcompete the surface reoxidation reaction. The dissolution of reoxidized surface Fe(III) is promoted by siderophores in a slow ligand controlled dissolution reaction with similar rates as the dark reaction. In solution, Fe(II)–siderophore complexes are oxidized immediately to Fe(III)–siderophore complexes by oxygen.

oxide surfaces in the presence of oxalate, non-steady-state dissolution experiments were performed. Goethite and lepidocrocite suspensions were irradiated in the presence of oxalate before adding the siderophore DFOB (Fig. 7A–C). The accumulation of labile surface sites is expected to result in a fast non-steady-state dissolution reaction after the addition of the siderophore. Accumulation and fast non-steady-state release of labile Fe(III) surface sites have been observed previously in thermal dissolution experiments involving oxalate and DFOB (Reichard et al., submitted for publication). Furthermore, a labilizing effect of light on the dissolution of colloidal iron oxides by unknown organic chromophores in seawater has been observed by Wells and Mayer (1991). We did not observe such a light-induced labilization of surface sites on goethite and lepidocrocite in the presence of oxalate. The sudden increase in dissolved iron, which occurred upon addition of DFOB to an aerated and irradiated goethite/oxalate suspension (Fig. 7C), is most likely due to the labilizing effect

of oxalate during the conditioning phase in the dark (17 h). The thermal formation of about 0.3–0.4 μM kinetically labile surface iron by oxalate is consistent with the results by Reichard et al. (submitted for publication).

5. Conclusions

Considering that the deposition of atmospheric aerosols to ocean waters may provide a significant source of iron in the form of solid oxides, photo-dissolution processes may be important for increasing the bioavailability of iron to the marine biota. According to our laboratory study, siderophores, including a nonphotoreductive siderophore, greatly accelerate light-induced dissolution of crystalline iron oxides. Addition of a second organic ligand, acting as the electron donor, further accelerates the dissolution process. This synergistic effect of siderophores and photoreductive ligands may be an important process in iron solubilization in iron-deficient marine surface waters, where photoreductive ligands as well as siderophores are present (Kuma et al., 1992; Nakabayashi et al., 1993; Van den Berg, 1995; Sempere and Kawamura, 1996; Macrellis et al., 2001).

Acknowledgements

We appreciate the technical assistance of Kurt Barmettler and Hans-Ueli Laubscher. Financial support was obtained from the Swiss Federal Institute for Environmental Science and Technology (EAWAG) and from Prof. Ruben Kretzschmar (Institute of Terrestrial Ecology).

References

- Abrahamson, H.B., Rezvani, A.B., Brushmiller, J.G., 1994. Photochemical and spectroscopic studies of complexes of iron(III) with citric-acid and other carboxylic-acids. *Inorg. Chim. Acta* 226, 117–127.
- Albrecht-Gary, A.M., Crumbliss, A.L., 1998. Coordination chemistry of siderophores: thermodynamics and kinetics of iron chelation and release. In: Sigel, A., Sigel, H. (Eds.), *Iron Transport and Storage in Microorganisms, Plants and Animals, Metal Ions in Biological Systems*, vol. 35. Marcel Dekker, New York, pp. 239–327.
- Anderson, M.A., Morel, F.M.M., 1982. The influence of aqueous iron chemistry on the uptake of iron by the coastal diatom *Thalassiosira-weissflogii*. *Limnol. Oceanogr.* 27, 789–813.
- Banwart, S., Davies, S., Stumm, W., 1989. The role of oxalate in accelerating the reductive dissolution of hematite ($\alpha\text{-Fe}_2\text{O}_3$) by ascorbate. *Colloid Surf.* 39, 303–309.
- Barbeau, K., Rue, E.L., Bruland, K.W., Butler, A., 2001. Photochemical cycling of iron in the surface ocean mediated by microbial iron(III)-binding ligands. *Nature* 413, 409–413.
- Barbeau, K., Zhang, G.P., Live, D.H., Butler, A., 2002. Petrobactin, a photoreactive siderophore produced by the oil-degrading marine bacterium *Marinobacter hydrocarbonoclasticus*. *J. Am. Chem. Soc.* 124, 378–379.
- Barbeau, K., Rue, E.L., Trick, C.G., Bruland, K.T., Butler, A., 2003. Photochemical reactivity of siderophores produced by marine heterotrophic bacteria and cyanobacteria based on characteristic Fe(III) binding groups. *Limnol. Oceanogr.* 48, 1069–1078.
- Bergeron, R.J., Huang, G.F., Smith, R.E., Bharti, N., McManis, J.S., Butler, A., 2003. Total synthesis and structure revision of petrobactin. *Tetrahedron* 59, 2007–2014.
- Bondiatti, C.G., 1992. Einfluss ausgewählter Liganden auf die Auflösungskinetik von Lepidokrokit ($\gamma\text{-FeOOH}$). PhD thesis, no. 9723, ETH Zürich.
- Brauer, G., 1963. *Handbuch der präparativen anorganischen Chemie*, Band II. Ferd. Enke Verlag, Stuttgart.
- Cheah, S.F., Kraemer, S.M., Cervini-Silva, J., Sposito, G., 2003. Steady-state dissolution kinetics of goethite in the presence of desferrioxamine B and oxalate ligands: implications for the microbial acquisition of iron. *Chem. Geol.* 198, 63–75.
- Cocozza, C., Tsao, C.C.G., Cheah, S.F., Kraemer, S.M., Raymond, K.N., Miano, T.M., Sposito, G., 2002. Temperature dependence of goethite dissolution promoted by trihydroxamate siderophores. *Geochim. Cosmochim. Acta* 66, 431–438.
- Duckworth, O.W., Martin, S.T., 2001. Surface complexation and dissolution of hematite by $\text{C}_1\text{--}\text{C}_6$ dicarboxylic acids at $\text{pH}=5.0$. *Geochim. Cosmochim. Acta* 65, 4289–4301.
- Faust, B.C., Hoffmann, M.R., 1986. Photoinduced reductive dissolution of $\alpha\text{-Fe}_2\text{O}_3$ by bisulfite. *Environ. Sci. Technol.* 20, 943–948.
- Finden, D.A.S., Tipping, E., Jaworski, G.H.M., Reynolds, C.S., 1984. Light-induced reduction of natural iron(III) oxide and its relevance to phytoplankton. *Nature* 309, 783–784.
- Furrer, G., Stumm, W., 1986. The coordination chemistry of weathering. I: dissolution kinetics of $\delta\text{-Al}_2\text{O}_3$ and BeO. *Geochim. Cosmochim. Acta* 50, 1847–1860.
- Gonye, E.R., Carpenter, E.J., 1974. Production of iron-binding compounds by marine microorganisms. *Limnol. Oceanogr.* 19, 840–842.
- Harris, W.R., Carrano, C.J., Raymond, K.N., 1979. Coordination chemistry of microbial iron transport compounds: 16. Isolation, characterization, and formation-constants of ferric aerobactin. *J. Am. Chem. Soc.* 101, 2722–2727.
- Haygood, M.G., Holt, P.D., Butler, A., 1993. Aerobactin production by a planktonic marine *Vibrio* sp. *Limnol. Oceanogr.* 38, 1091–1097.

- Hersman, L., Lloyd, T., Sposito, G., 1995. Siderophore-promoted dissolution of hematite. *Geochim. Cosmochim. Acta* 59, 3327–3330.
- Hutchins, D.A., Witter, A.E., Butler, A., Luther, G.W., 1999. Competition among marine phytoplankton for different chelated iron species. *Nature* 400, 858–861.
- Johansen, A.M., Siefert, R.L., Hoffmann, M.R., 2000. Chemical composition of aerosols collected over the tropical North Atlantic Ocean. *J. Geophys. Res.* 105, 15277–15312.
- Johnson, K.S., Coale, K.H., Elrod, V.A., Tindale, N.W., 1994. Iron photochemistry in seawater from the equatorial Pacific. *Mar. Chem.* 46, 319–334.
- Jones, G.J., Palenik, B.P., Morel, F.M.M., 1987. Trace-metal reduction by phytoplankton—the role of plasmalemma redox enzymes. *J. Phycol.* 23, 237–244.
- Kraemer, S.M., 2004. Iron oxide dissolution and solubility in the presence of siderophores. *Aquat. Sci.* 66, 3–18.
- Kuma, K., Nakabayashi, S., Suzuki, Y., Kudo, I., Matsunaga, K., 1992. Photo-reduction of Fe(III) by dissolved organic substances and existence of Fe(II) in seawater during spring blooms. *Mar. Chem.* 37, 15–27.
- Kuma, K., Nakabayashi, S., Matsunaga, K., 1995. Photoreduction of Fe(III) by hydroxycarboxylic acids in seawater. *Water Res.* 29, 1559–1569.
- Litter, M.I., Blesa, M.A., 1988. Photodissolution of iron-oxides: 1. Maghemite in EDTA solutions. *J. Colloid Interface Sci.* 125, 679–687.
- Liu, X.W., Millero, F.J., 2002. The solubility of iron in seawater. *Mar. Chem.* 77, 43–54.
- Macrellis, H.M., Trick, C.G., Rue, E.L., Smith, G., Bruland, K.W., 2001. Collection and detection of natural iron-binding ligands from seawater. *Mar. Chem.* 76, 175–187.
- Maldonado, M.T., Price, N.M., 1999. Utilization of iron bound to strong organic ligands by plankton communities in the subarctic Pacific Ocean. *Deep-Sea Res. II* 46, 2447–2473.
- Maldonado, M.T., Price, N.M., 2001. Reduction and transport of organically bound iron by *Thalassiosira oceanica* (Bacillariophyceae). *J. Phycol.* 37, 298–309.
- Martell, A.E., Smith, R.M., Motekaitis, R.J., 2001. NIST Critically Selected Stability Constants of Metal Database. NIST, Gaithersburg.
- Martin, J.H., Fitzwater, S.E., 1988. Iron-deficiency limits phytoplankton growth in the northeast Pacific Subarctic. *Nature* 331, 341–343.
- Martin, J.H., Gordon, R.M., Fitzwater, S., Broenkow, W.W., 1989. VERTEX: phytoplankton/iron studies in the Gulf of Alaska. *Deep-Sea Res.* 36, 649–680.
- Martin, J.H., Coale, K.H., Johnson, K.S., Fitzwater, S.E., Gordon, R.M., Tanner, S.J., Hunter, C.N., Elrod, V.A., Nowicki, J.L., Coley, T.L., Barber, R.T., Lindley, S., Watson, A.J., Vanscoy, K., Law, C.S., Liddicoat, M.I., Ling, R., Stanton, T., Stockel, J., Collins, C., Anderson, A., Bidigare, R., Ondrusek, M., Latasa, M., Millero, F.J., Lee, K., Yao, W., Zhang, J.Z., Friederich, G., Sakamoto, C., Chavez, F., Buck, K., Kolber, Z., Greene, R., Falkowski, P., Chisholm, S.W., Hoge, F., Swift, R., Yungel, J., Turner, S., Nightingale, P., Hatton, A., Liss, P., Tindale, N.W., 1994. Testing the iron hypothesis in ecosystems of the equatorial Pacific-Ocean. *Nature* 371, 123–129.
- Miller, W.L., Kester, D., 1994. Photochemical iron reduction and iron bioavailability in seawater. *J. Mar. Res.* 52, 325–343.
- Millero, F.J., Sotolongo, S., Izaguirre, M., 1987. The oxidation kinetics of Fe(II) in seawater. *Geochim. Cosmochim. Acta* 51, 793–801.
- Nakabayashi, S., Kudo, I., Kuma, K., Matsunaga, K., Hasebe, K., 1993. Trace determination of sugar acids (gluconic acid) in sea water by liquid-chromatography. *Anal. Chim. Acta* 271, 25–29.
- Pehkonen, S.O., Siefert, R., Erel, Y., Webb, S., Hoffmann, M.R., 1993. Photoreduction of iron oxyhydroxides in the presence of important atmospheric organic compounds. *Environ. Sci. Technol.* 27, 2056–2062.
- Powell, R.T., Donat, J.R., 2001. Organic complexation and speciation of iron in the South and Equatorial Atlantic. *Deep-Sea Res. II* 48, 2877–2893.
- Reichard, P.U., Kretzschmar, R., Kraemer, S.M., 2004. Non-steady state dissolution mechanism of goethite in the presence of siderophores and organic acids (submitted for publication).
- Reid, R.T., Butler, A., 1991. Investigation of the mechanism of iron acquisition by the marine bacterium *Alteromonas luteoviolacea*: characterization of siderophore production. *Limnol. Oceanogr.* 36, 1783–1792.
- Rich, H.W., Morel, F.M.M., 1990. Availability of well-defined iron colloids to the marine diatom *Thalassiosira weissflogii*. *Limnol. Oceanogr.* 35, 652–662.
- Rue, E.L., Bruland, K.W., 1997. The role of organic complexation on ambient iron chemistry in the equatorial Pacific Ocean and the response of a mesoscale iron addition experiment. *Limnol. Oceanogr.* 42, 901–910.
- Schwertmann, U., Cornell, R.M., 1991. Iron Oxides in the Laboratory. VCH, Weinheim.
- Sempere, R., Kawamura, K., 1996. Low molecular weight dicarboxylic acids and related polar compounds in the remote marine rain samples collected from western Pacific. *Atmos. Environ.* 30, 1609–1619.
- Sempere, R., Kawamura, K., 2003. Trans-hemispheric contribution of C₂–C₁₀ α, ω-dicarboxylic acids, and related polar compounds to water-soluble organic carbon in the western Pacific aerosols in relation to photochemical oxidation reactions. *Glob. Biogeochem. Cycles* 17, 1069. doi:10.1029/2002GB001980.
- Siefert, R.L., Pehkonen, S.O., Erel, Y., Hoffmann, M.R., 1994. Iron photochemistry of aqueous suspensions of ambient aerosol with added organic acids. *Geochim. Cosmochim. Acta* 58, 3271–3279.
- Siffert, C., Sulzberger, B., 1991. Light-induced dissolution of hematite in the presence of oxalate: a case-study. *Langmuir* 7, 1627–1634.
- Soria-Dengg, S., Horstmann, U., 1995. Ferrioxamine-B and ferrioxamine-E as iron sources for the marine diatom *Phaeodactylum tricorutum*. *Mar. Ecol., Prog. Ser.* 127, 269–277.
- Stumm, W., Sulzberger, B., 1992. The cycling of iron in natural environments: considerations based on laboratory studies of heterogeneous redox processes. *Geochim. Cosmochim. Acta* 1, 3233–3257.

- Stumm, W., Kummert, R., Sigg, L., 1980. A ligand-exchange model for the adsorption of inorganic and organic-ligands at hydrous oxide interfaces. *Croat. Chem. Acta* 53, 291–312.
- Sulzberger, B., Laubscher, H., 1995a. Photochemical reductive dissolution of lepidocrocite—effect of pH. In: Huang, C.P., O'Melia, C.R., Morgan, J.J. (Eds.), *Aquatic Chemistry, Interfacial and Interspecies Processes*, Adv. Chem. Ser., vol. 244. American Chemical Society, Washington, DC, pp. 279–290.
- Sulzberger, B., Laubscher, H., 1995b. Reactivity of various types of iron(III) (hydr)oxides towards light-induced dissolution. *Mar. Chem.* 50, 103–115.
- Taylor, S.W., Luther, G.W., Waite, J.H., 1994. Polarographic and spectrophotometric investigation of iron(III) complexation to 3,4-dihydroxyphenylalanine-containing peptides and proteins from *Mytilus edulis*. *Inorg. Chem.* 33, 5819–5824.
- Tortell, P.D., Maldonado, M.T., Granger, J., Price, N.M., 1999. Marine bacteria and biogeochemical cycling of iron in the oceans. *FEMS Microbiol. Ecol.* 29, 1–11.
- Van den Berg, C.M.G., 1995. Evidence for organic complexation of iron in seawater. *Mar. Chem.* 50, 139–157.
- Verweij, W., 1999–2001. CHEAQS (a program for calculating chemical equilibria in aquatic systems). Vers. L19, The Netherlands.
- Voelker, B.M., Morel, F.M.M., Sulzberger, B., 1997. Iron redox cycling in surface waters: effects of humic substances and light. *Environ. Sci. Technol.* 31, 1004–1011.
- Waite, T.D., Morel, F.M.M., 1984. Photoreductive dissolution of colloidal iron oxide: effect of citrate. *J. Colloid Interface Sci.* 102, 121–137.
- Weger, H.G., 1999. Ferric and cupric reductase activities in the green alga *Chlamydomonas reinhardtii*: experiments using iron-limited chemostats. *Planta* 207, 377–384.
- Welch, K.D., Davis, T.Z., Aust, S.D., 2002. Iron autoxidation and free radical generation: effects of buffers, ligands, and chelators. *Arch. Biochem. Biophys.* 397, 360–369.
- Wells, M.L., 1999. Manipulating iron availability in nearshore waters. *Limnol. Oceanogr.* 44, 1002–1008.
- Wells, M.L., Mayer, L.M., 1991. The photoconversion of colloidal iron oxyhydroxides in seawater. *Deep-Sea Res.* 38, 1379–1395.
- Wells, M.L., Zorkin, N.G., Lewis, A.G., 1983. The role of colloid chemistry in providing a source of iron to phytoplankton. *J. Mar. Res.* 41, 731–746.
- Wells, M.L., Price, N.M., Bruland, K.W., 1994. Iron limitation and the *Cyanobacterium synechococcus* in equatorial Pacific waters. *Limnol. Oceanogr.* 39, 1481–1486.
- Wilhelm, S.W., Trick, C.G., 1994. Iron-limited growth of cyanobacteria: multiple siderophore production is a common response. *Limnol. Oceanogr.* 39, 1979–1984.
- Winkelman, G., 1991. *Handbook of Microbial Iron Chelates*. CRC Press, Boca Raton, FL.
- Witter, A.E., Hutchins, D.A., Butler, A., Luther, G.W., 2000. Determination of conditional stability constants and kinetic constants for strong model Fe-binding ligands in seawater. *Mar. Chem.* 69, 1–17.
- Wu, J.F., Luther, G.W., 1995. Complexation of Fe(III) by natural organic-ligands in the northwest Atlantic-ocean by a competitive ligand equilibration method and a kinetic approach. *Mar. Chem.* 50, 159–177.
- Yoshida, T., Hayashi, K., Ohmoto, H., 2002. Dissolution of iron hydroxides by marine bacterial siderophore. *Chem. Geol.* 184, 1–9.
- Zhu, X., Prospero, J.M., Savoie, D.L., Millero, F.J., Zika, R.G., Saltzman, E.S., 1993. Photoreduction of iron(III) in marine mineral aerosol solutions. *J. Geophys. Res.* 98, 9039–9046.
- Zinder, B., Furrer, G., Stumm, W., 1986. The coordination chemistry of weathering: II. Dissolution of Fe(III) oxides. *Geochim. Cosmochim. Acta* 50, 1861–1869.